

Photoluminescent carbon colloids prepared by laser fragmentation of carbon from waste coffee grounds

N. Enríquez-Sánchez, A.R. Vilchis-Nestor, S. Camacho-López, M.A. Camacho-López, M. Camacho-López

Colloidal suspensions of carbon nanostructures (CNSs) were prepared by laser fragmentation in various liquid media using heat-treated coffee grounds as carbon precursor. A study by calorimetry was done in powder of waste coffee grounds to determine the temperature of obtaining carbon. The experiments were carried out in two stages, the first one consisted in obtaining the carbon source, for which powder of waste coffee grounds was thermally treated in air. The as-obtained carbon was characterized by scanning electron microscopy, energy dispersive X-ray spectroscopy, Raman spectroscopy and infrared spectroscopy. In the second step the as-obtained carbon was separately dispersed in four liquid media (acetone, toluene, methanol and isopropyl alcohol) to be fragmented by using a ns-pulsed Nd:YAG laser at its 1064 nm fundamental emission. The morphological features of the carbon nanostructures were obtained by transmission electron microscopy, while the optical properties of the colloidal suspensions were characterized by UV-Vis and photoluminescence spectroscopies. Results indicate that carbon nanostructures are successfully obtained in the four liquid media after the fragmentation process. The four colloidal suspensions show photoluminescent properties, which are seen to depend on the liquid medium nature. We found that the liquid medium also influences the efficiency of the laser fragmentation.

Introduction

Coffee is one of the most important agro-industrial products worldwide, in 2021 there was a production of 10.2 million tons [1]. Likewise, it is estimated that for each kilogram of coffee grains between 330 and 450 g of instant coffee are produced, which generates between 670 and 550 g of spent coffee (waste coffee) [2], which is highly polluting due to the large amount of organic matter that it contains, which is of low biodegradability. Waste coffee is lignocellulosic biomass, which is essentially composed of carbon, oxygen, hydrogen, and nitrogen. It contains cellulose between 59.2 and 62.94%, hemicellulose between 5 and 10% and lignin between 19.8 and 26.5%. In addition, this type of waste usually has some inorganic elements considered as micronutrients such as calcium, magnesium, or sodium, but their concentrations are generally less than 5% [3].

According to P. Jagdale *et al.* [4] the pyrolysis process of coffee waste takes place in three stages of decomposition. The first one occurs from 25 to 200 °C, which corresponds to a mass loss of 9% due to dehydration and a slight release of volatile organic compounds. The second one occurs between 200 and 500 °C, which is associated with the greatest mass loss of around 71%, which is attributed to the decomposition of its main constituents (cellulose, hemicellulose, and lignin). The third step takes place from 500 to 700 °C and is due to the decomposition of the remaining biomass and the formation of ash.

The main uses of waste coffee are the production of biofuels, activated carbons, sensors, and as a material in the production of electrodes for Li-ion batteries and capacitors, as well as in the synthesis of quantum carbon dots, among others [5-8]. The peculiar optical properties of some carbon-based nanomaterials have attracted much interest for a wide variety of biomedical applications, due to their low toxicity and excellent biocompatibility. As an example of its application in this field, the use of Carbon-Graphene Quantum Dots (C-GQDs) for Parkinson's disease was investigated in primary neurons has been proposed [8].

The synthesis of carbon nanosheets by means of laser ablation has already been reported by using pyrolytic graphite target as carbon precursor [9]. The use of waste biomaterials, such as the peels and seeds of fruits and vegetables is an ecological alternative for the production of carbon-based nanomaterials [10,11]. In addition, this type of synthesis of materials is convergent with the current growing demand for a circular economy.

In this work, we demonstrate a facile method for the obtaining of photoluminescent colloidal suspensions of carbon nanostructures, by using laser fragmentation of the carbon particles precursor obtained from waste coffee. We prepare colloidal suspensions in various liquid media to investigate its influence on the precursor fragmentation


Noé Enríquez-Sánchez [‡], Marco Camacho-López 

Laboratorio de Investigación y Desarrollo de Materiales Avanzados,
Facultad de Química, Universidad Autónoma del Estado de México
Toluca, Edo. Mex., 50200, México.

[‡] Doctorado en Ciencia de Materiales, Facultad de Química,
Universidad Autónoma del Estado de México
Toluca, Edo. Mex., 50120, México.

Alfredo R. Vilchis-Nestor 

Centro Conjunto de Investigación en Química Sustentable UAEM-UNAM,
Facultad de Química, Universidad Autónoma del Estado de México
Toluca, Edo. Mex., 50200, México.

Santiago Camacho-López 

Departamento de Óptica,
Centro de Investigación Científica y de Educación Superior de Ensenada
Ensenada, B.C., 22860, México.

Miguel A. Camacho-López

Lab. de Fotomedicina, Biofotónica y Espectroscopía Láser de Pulsos
Ultracortos, Fac. Medicina, Universidad Autónoma del Estado de México
Toluca, Edo. Mex., 50120, México.

Received: May 17th, 2024

Accepted: September 11th, 2024

Published: September 30th, 2024

© 2024 by the authors. Creative Commons Attribution

https://doi.org/10.47566/2024_syv37_1-240901

efficiency and on the various characteristics of the CNSs including their photoluminescence properties.

Materials and Methods

Laser fragmentation

The preparation of the colloidal suspensions of carbon nanostructures was carried out in two stages. First, it was necessary to obtain the carbon precursor from the waste coffee. 1.5 g of waste coffee was placed in a tubular oven (HT-1100D25, Evlesa). A thermal treatment was carried out at 400 °C for 30 min in air. In Figure 1a we can see the starting waste coffee material that was used as well as the product obtained after the heat treatment. The material changed from brown to black through the heat treatment. After every carbonization process, the black product obtained was mechanically pulverized to get a fine powder. Subsequently, colloidal suspensions of carbon nanostructures in acetone (Fermont), toluene (Wöhler), methanol (Fermont) and isopropyl alcohol (Fermont) were prepared by laser fragmentation as it is shown in Figure 1b, for this, 20 mg of calcined waste coffee were placed in a glass vial and 20 mL of liquid medium was added on it. The mixture carbon powder-liquid medium was irradiated for 15 min with 7 ns laser pulses of a Nd:YAG laser (Minilite II, Continuum) whose emission is at 1064 nm, and a repetition rate of 15 Hz. The laser pulses were focused down by using a lens of 30 cm focal length, giving a per pulse laser fluence of 1.6 J/cm². The vial was in constant motion in order to avoid irradiation at the same fixed spot and therefore aiming for maximizing the amount of fragmented material during the ablation process.

Figure 1c shows photographs of the colloidal suspensions obtained immediately after laser fragmentation, and also 24 h and 100 days after. Following laser fragmentation a large portion of the colloidal material rapidly precipitates for toluene and methanol, giving rise to light brownish colloidal suspensions. On the contrary, when acetone and isopropyl alcohol are used in the colloidal suspensions these show a dark brown color, which indicates a better stability. Notice that after 24 h, to obtain a colloidal suspension the

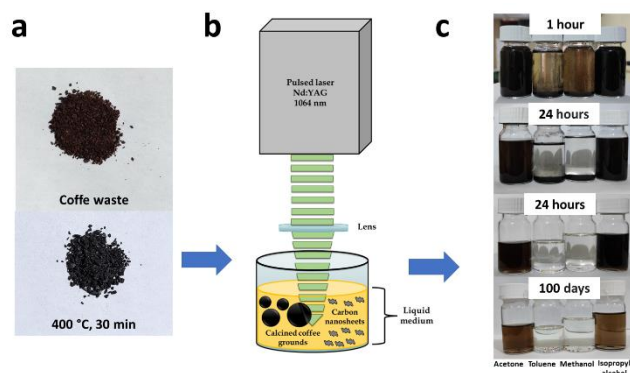


Figure 1. Experimental scheme for the synthesis of carbon nanostructures obtained from coffee waste by laser fragmentation. a) Coffee waste before and after heat treatment at 400 °C for 30 minutes, b) experimental setup for the fragmentation process, c) colloidal suspensions of carbon nanostructures obtained on the day of fragmentation (0 days), 24 hours and 100 days after fragmentation.

sedimented material in the samples was removed. Long after synthesis, i.e. at 100 days from the laser fragmentation, the four colloidal suspensions remain remarkably stable.

Characterization

Waste coffee was analyzed by differential scanning calorimetry, thermogravimetry and infrared spectroscopy. The calcined waste coffee was morphologically and structurally characterized by scanning electron microscopy (SEM), Raman and infrared spectroscopies. The morphological and structural characterization of the carbon nanostructures was obtained by transmission electron microscopy (TEM), while the optical properties of the colloidal suspensions of carbon nanostructures were characterized by UV-Vis and photoluminescence spectroscopies. Differential scanning calorimetry and thermogravimetry analyzes were performed in a simultaneous thermal analyzer (STA 8000, PerkinElmer). Measurements were made in the temperature range from room temperature up to 800 °C with a heating rate of 10 °C/min, under a nitrogen atmosphere. The morphological characterization of the calcined waste coffee was carried out using a scanning electron microscope (JEOL JSM-6510LV) with an acceleration voltage of 20 kV, which is coupled with an X-ray detector (Oxford) for chemical analysis by energy dispersive X-ray spectroscopy (EDS). Image acquisition and EDS analysis were performed on a micrometric powder sample of calcined waste coffee on copper tape. Fourier transform infrared spectra were run on an IR spectrometer (IRPrestige-21, Shimadzu) from 600 to 4000 cm⁻¹, for waste coffee before and after heat treatment. Raman characterization was performed with a Raman spectrometer (Xplora Plus, Jobin-Yvon-Horiba), using a laser with a wavelength of 532 nm. A laser beam delivering 2.5 mW power was focused on the sample with a 50X objective lens. UV-Vis spectroscopy analysis of the obtained colloidal suspensions was performed using a double-beam spectrophotometer (Lambda 650, Perkin-Elmer), within the 200 to 850 nm range. A quartz cuvette with an optical path length of 10 mm was used for characterization. For UV-Vis spectroscopy analyses, 2 mL of the colloidal suspension was diluted by adding 4 mL of liquid medium. UV-Vis spectra were obtained by placing 3.5 mL of the diluted colloidal suspension. Photoluminescence spectroscopy analyzes were performed for the obtained colloidal suspensions by using a spectrofluorometer (Fluoromax-p, Jobin-Yvon-Horiba). Emission spectra were also obtained by placing 3.5 mL of the diluted colloidal suspension in a quartz cuvette with a 10 mm optical path length. The morphological and structural characterization of the fragmented carbon was performed in a transmission electron microscope (JEOL 2100) with an acceleration voltage of 200 kV. The TEM image acquisition was performed on samples prepared by evaporation at room temperature of a drop of the colloidal suspension on a grid.

Results and discussion

Figure 2 shows the results obtained from the calorimetric analysis. The TGA curve shows the weight loss of waste

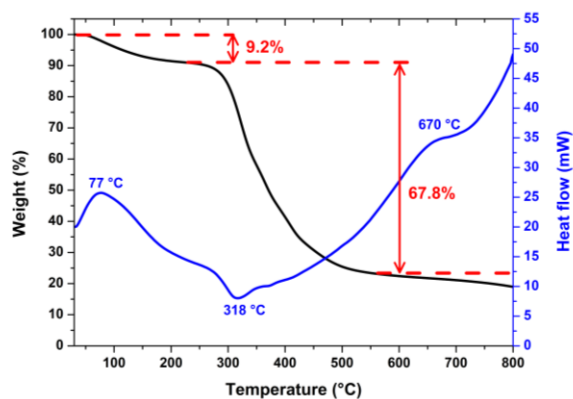


Figure 2. Thermal analyzes of waste coffee.

coffee when it is heating up to 800 °C. There are clearly three stages of weight loss; the first one below 200 °C corresponds to water evaporation in the sample (sample dehydration) with a weight loss of 9.2% [12]; the second stage corresponds to the greatest weight loss, and it takes place between 200 and 500 °C, this weight loss of around 67.8% is related to the decomposition of the main constituents of waste coffee such as hemicellulose, cellulose and some fraction of lignin. Hemicellulose degradation occurs between 200 and 300 °C, followed by cellulose degradation between 300 and 400 °C, and finally lignin degradation that occurs above 400 °C [13]; the last stage occurs after 500 °C, and corresponds to the decomposition of the remaining biomass [4]. The DSC thermogram shows the temperature transitions of the sample between 30 and 800 °C. The thermogram obtained shows three main events, the first of which is an endothermic event with a peak around 77 °C, this event is related to water vaporization in the sample, which indicates the presence of hydrophilic groups [12]. The second event that is observed around 318 °C is an exothermic transition, this event is related to the thermal decomposition of the sample [14]. The third event is a small endothermic peak can be observed near 670 °C attributed to the secondary pyrolysis of lignin [15].

Figure 3a shows a SEM image of the carbon obtained from waste coffee, we can see micrometer-sized particles in the form of scales, the elemental analysis by EDS (Figure 3b) shows that the material is mainly constituted by carbon and oxygen, as well as small amounts of calcium and magnesium.

Figure 4 shows the infrared spectra of the waste coffee before and after the heat treatment. For coffee waste without heat treatment, one can see a broad band around 3315 cm^{-1}

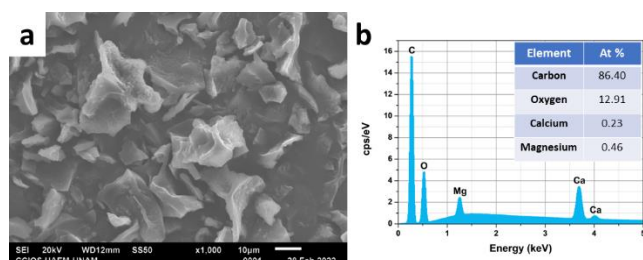


Figure 3. a) SEM image and b) EDS spectrum of waste coffee thermally treated at 400 °C for 30 minutes.

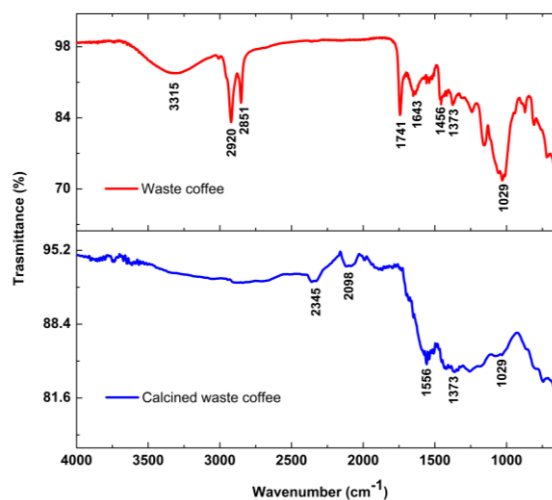


Figure 4. Infrared spectra of waste coffee before and after heat treatment.

which is due to the stretching vibration of the hydroxyl groups (alcohols, sugars, phenols, and carboxylic acids), as well as water adsorbed on the surface [16]. The signals at 2920 and 2851 cm^{-1} are assigned to the asymmetric and symmetric stretches of aliphatic CH, respectively. The signal at 1741 cm^{-1} is due to the axial deformation of the C=O bond of esters. The signal at 1643 cm^{-1} is attributed to stretching of the C=C bond of aromatic compounds. The signal at 1456 cm^{-1} is associated with the asymmetric deformation of the aliphatic CH bond. The signal at 1373 cm^{-1} and the band at 1029 cm^{-1} are due to stretching and deformation of the CO bond, respectively [17]. If we compare the infrared spectrum of heat-treated waste coffee, against the one of the nontreated waste coffee, it can be seen that most of the starting spectral features have disappeared, this is because between 200 and 500 °C the decomposition of the main constituents of coffee waste takes place (cellulose, hemicellulose and lignin) [4]. Notice, though, the appearance of two new signals at 2345 and 2098 cm^{-1} which are associated to the presence of carbon dioxide and carbon monoxide, respectively [18]. The signal at 1556 cm^{-1} is due to stretching of the aromatic ring C=C [19]. Notice that the intensity of the signals at 1373 and 1029 cm^{-1} associated to the stretching and deformation of the CO bond have decreased.

Figure 5 shows the Raman spectrum of calcined waste coffee, which shows two signals, the D band at 1357 cm^{-1} and the G band at 1575 cm^{-1} . The D band is assigned to disorder originated from sp^3 hybridized carbons, while the G band is associated with a hexagonal carbon structure [20]. The relationship between the intensities of the D and G bands (I_D/I_G) is related to the degree of structural disorder [21]. By means of a Lorentzian fit to the Raman spectrum, we obtained a $I_D/I_G = 1.02$ value, indicating a high degree of disorder.

Figure 6 shows the optical absorption spectra of the obtained colloidal suspensions in each of the liquid medium. The UV-Vis measurements were performed the same day of the laser fragmentation experiments. It is possible to observe that colloidal suspensions obtained in acetone and isopropyl alcohol present the highest absorbance values in the 400 -

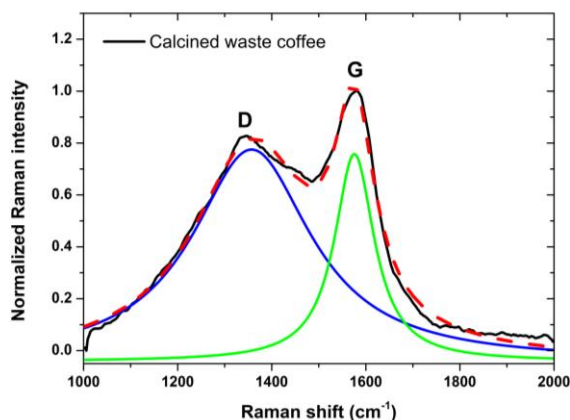


Figure 5. Raman spectrum of carbon obtained from the calcination of waste coffee. Also, Lorentzian curves from the deconvolution of Raman spectrum are included.

850 nm region, while the colloidal suspensions obtained in toluene and methanol present the lowest absorbance values, which indicates that there is a larger amount of fragmented material in the case of acetone and isopropyl alcohol, in good agreement with what is shown in Figure 1c. Therefore, we can conclude that the liquid medium influences the efficiency of the fragmentation, being more efficient in the case of acetone and isopropyl alcohol.

Figure 7(a-b) show photographs of the carbon colloidal suspensions under white and ultraviolet light ($\lambda = 370$ nm) illumination, respectively. Figure 7c shows the photoluminescence emission spectra of the colloidal suspensions of carbon in each one of the liquid media, which were obtained at an excitation wavelength of 370 nm. The photoluminescence measurements were performed the same day of the laser fragmentation experiments. By observing the photoluminescence emission spectra, it is possible to see that the colloidal suspensions that show the higher photoluminescence emission are those obtained in toluene and methanol, while in the case of acetone and isopropyl alcohol the intensity is lower, which is in good agreement with what is shown in Figure 7b. These results seem to contradict what was expected based on the colloidal suspension concentrations, i. e. one can expect that at higher

concentrations the photoluminescence emission would be higher, however, in photoluminescence spectroscopy, the observed intensity of fluorescence is not proportional to the concentration of the analyte, this is due to the fact that there is a good amount of absorption of the incident and emission radiation propagating through the analyte. This phenomenon is known as the internal filter effect (IFE). One way to deal with IFE is to dilute samples to low enough concentrations such that the IFE contribution is negligible and the fluorescence intensity is linearly dependent on the analyte concentration. It is important to consider that to do dilutions can be a tedious and error-prone activity. Furthermore, the dilution can also affect the molecular property of the condensed state, such as binding, solvation, and degree of association, that would otherwise be present in a higher concentration range. The best accepted method for dealing with IFE effects is the use of mathematical correction models [22].

In our case, by having two quite concentrated colloidal suspensions, i. e. carbon nanostructures in acetone and isopropyl alcohol, their recorded luminescence intensity is strongly affected by the IFE. On the contrary for the case of the colloidal suspensions in toluene and methanol, the concentration of carbon nanostructures is quite low, such that there is no IFE that affects the photoluminescence emission. This makes no possible to directly compare the photoluminescence emission intensity between the four colloidal suspensions. For this reason, in the future, it would be important to implement both experimental methods and mathematical models that enable an adequate comparison of the photoluminescent features of the colloidal suspensions of carbon nanostructures obtained through the laser fragmentation of carbon.

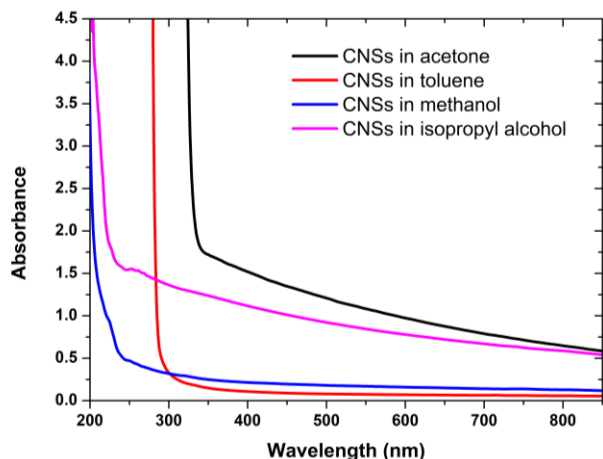


Figure 6. UV-vis spectra of the colloidal solutions obtained.

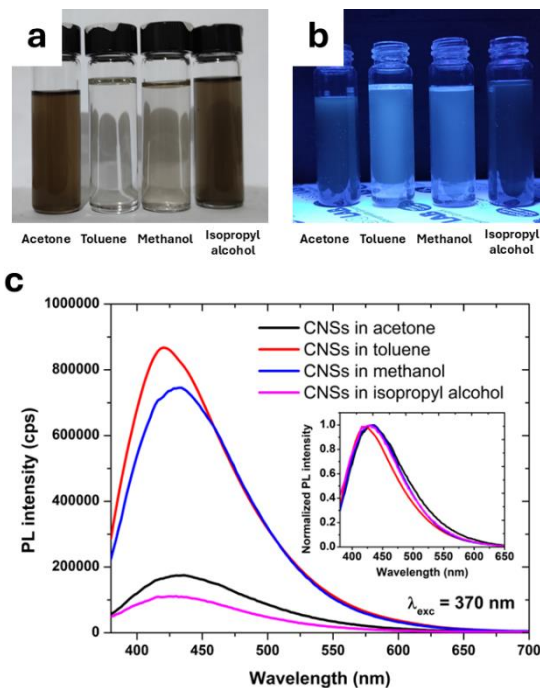


Figure 7. Photographs of the colloidal suspensions obtained under illumination with a) white light and b) ultraviolet light, respectively. c) Emission spectra obtained at an excitation wavelength of 370 nm.

The graph inserted in Figure 7c shows the normalized emission spectra of the four samples. The samples exhibit a broad photoluminescence emission spectrum centered around 430 nm when excited with a wavelength of 370 nm. In addition, slight changes in the shape and position of the emission bands can be observed. Owing to the presence of edge or surface states, the photoluminescence emission spectra of carbon nanomaterials are generally expected to be broad. The broad photoluminescence spectrum of carbon nanomaterials is an emission composed of aromatic domains, surface states, and various functional groups attached to the surface of the materials [23]. The use of residual biomass as a carbon source in the synthesis of carbon nanomaterials allows obtaining functionalized materials due to the presence of many organic compounds in the natural source [10,11]. Furthermore, during the synthesis and processing of nanomaterials by laser, part of the energy of the laser beam is given to the liquid medium allowing its decomposition which can lead to the functionalization of the materials obtained [24,25]. The emission of light by carbon nanomaterials may be due to size effects (quantum confinement), however, an alternative explanation assumes that the emission comes from functional groups attached to their surface (surface passivation). The presence of different functional groups on the surface of the materials originated during the fragmentation process can cause heterogeneity in the emission spectra. However, in order to establish a correlation between the differences in the photoluminescence emission spectra and the presence of different functional groups, further studies are required.

Figure 8 shows TEM images of the carbon nanostructures obtained from the fragmentation of calcined waste coffee in each of the liquid media (acetone, toluene, methanol and isopropyl alcohol). For the case of acetone Figure 8a, carbon

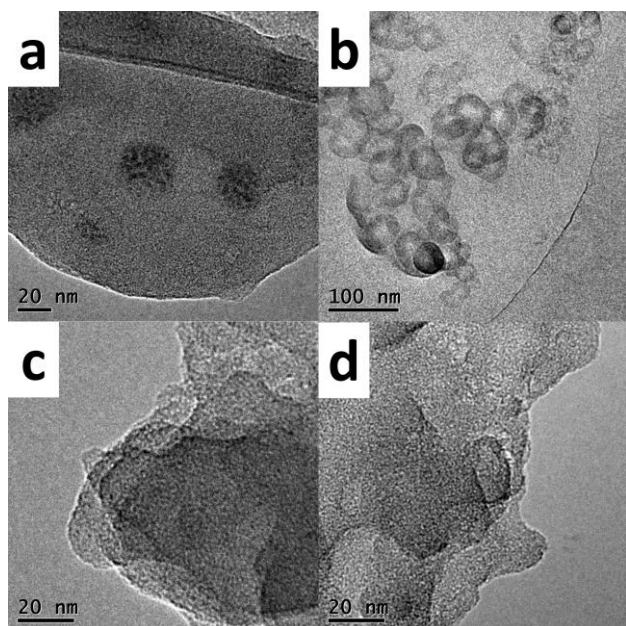


Figure 8. TEM image of the carbon nanostructures obtained after fragmentation in a) acetone, b) toluene, c) methanol and d) isopropyl alcohol.

nanoparticles embedded into nanosheets are obtained. In the case of acetone (Figure 8a) the spherical nanoparticles within the carbon nanosheets have an average size of 45 nm, which agrees well with what was previously reported by our group [26]. For toluene (Figure 8b) it is possible to observe that the fragmentation process generates spherical nanoparticles with an average size of 50 nm. When methanol and isopropyl alcohol are used (Figure 8, c and d), very good formation of nanosheets is obtained, however, for these liquid media there are no evidence of embedded nanoparticles. These results indicate that liquid media determine the type of nanostructures that result from the laser fragmentation. It can be either nanosheets with embedded nanoparticles, just nanoparticles, or nanoparticle free nanosheets.

Conclusions

A low cost, environmentally friendly and simple laser fragmentation method for the synthesis of carbon nanostructures has been demonstrated. Waste coffee is an abundant material that can be easily processed for the purpose of obtaining technologically usable products. The adequate heat treatment of waste coffee grounds provides an excellent carbon precursor for the synthesis of nanosheets with embedded nanoparticles, isolated nanoparticles or nanoparticle free nanosheets. The type of nanostructures that result of the laser fragmentation is determined by the liquid medium utilized for the laser fragmentation. We found also that the liquid medium, in this case, acetone, toluene, methanol and isopropyl alcohol, also influences the efficiency of the fragmentation process, significantly affecting the colloidal suspension concentration. All the colloidal suspensions of either nanosheets with embedded nanoparticles, isolated nanoparticles or nanoparticle free nanosheets show photoluminescence emission with wavelength centered (430 nm) in the blue spectral region, and a full width at half maximum of ~ 100 nm.

Acknowledgements

To M. C. M. Francisco Nieto and Dr. Enrique Viguera for the FTIR and calorimetry measurements. To Dr. Victor H. Castrejon for the Raman analyses. To CONACyT for the scholarship for postgraduate studies 789629.

Referencias

- [1]. A.I. Costa, P.D. Barata, B. Morales, J.V. Prata, *Chemosensors* **10**, 113 (2022).
- [2]. A.E. Atabani, S.M. Mercimek, S. Arvindnarayan, S. Shobana, G. Kumar, M. Cadir, A.H. Al-Muhateb, *J. Air Waste Manag. Assoc.* **68**, 196 (2018).
- [3]. F.J. Cerino-Córdova, N.E. Dávila-Guzmán, A.M. García León, J.J. Salazar-Rabago, E. Soto-Regalado, *Revalorization of Coffee Waste, in: Coffee-Production and Research*, Ed. D. T. Castanheira (IntechOpen, 2020), pp. 1-26.
- [4]. P. Jagdale, D. Ziegler, M. Rovere, J.M. Tulliani, A. Tagliaferro, *Sensors* **19**, 801 (2019).
- [5]. I.K. Kookos, *Resour. Conserv. Recycl.* **134**, 156 (2018).
- [6]. J. Ren, N. Chen, L. Wan, G. Li, T. Chen, F. Yang, S. Sun, *Molecules* **26**, 257 (2021).

- [7]. T.S. Andrade, J. Vakros, D. Mantzavinos, P. Lianos, *Chem. Eng. J. Adv.* **4**, 100061 (2020).
- [8]. D.J. Kim, J.M. Yoo, Y. Suh, D. Kim, I. Kang, J. Moon, M. Park, J. Kim, K.S. Kang, B.H. Hong, *Nanomaterials* **11**, 1423 (2021).
- [9]. L. Escobar Alarcón, M.E. Espinosa Pesqueira, D.A. Solis Casados, J. Gonzalo, J. Solis, M. Martínez Orts, E. Haro Poniowski, *Appl. Phys. A* **124**, 141 (2018).
- [10]. O.G. Rojas-Valencia, M. Regules-Carrasco, J. Hernández-Fuentes, C.M. Reza-San Germán, M. Estrada-Flores, E. Villagarcía-Chávez, *Materialia* **19**, 101182 (2021).
- [11]. O.G. Rojas-Valencia, D.L. Díaz-Santiago, J.L. Casas-Espínola, C.M. Reza-San Germán, M. Estrada Flores, *Inorg. Chem. Commun.* **158**, 111604 (2023).
- [12]. L.F. Ballesteros, J.A. Teixeira, S.I. Mussatto, *Food Bioproc. Tech.* **7**, 3493 (2014).
- [13]. A.C. Fonseca-Alves, R.V. Pacheco-Antero, S.B. de Oliveira, S.A. Ojala, P.S. Scalize, *Environ. Sci. Pollut. Res.* **26**, 24850 (2019).
- [14]. L.F. Ballesteros, J.A. Teixeira, S.I. Mussatto, *Carbohydr. Polym.* **157**, 258 (2017).
- [15]. H. Yang, R. Yan, H. Chen, D.H. Lee, C. Zheng, *Fuel* **86**, 1781 (2007).
- [16]. L. Hao, P. Wang, S. Valiyaveetil, *Sci. Rep.* **7**, 42881 (2017).
- [17]. R.M. Correia, L.B. Loureiro, R.R.T. Rodrigues, H.B. Costa, B.G. Oliveira, P.R. Filgueiras, C.J. Thompson, V. Lacerda, W. Romão, *Anal. Methods* **8**, 7678 (2016).
- [18]. B. Zapata, J. Balmaseda, E. Fregoso-Israel, E. Torres-García, *J. Therm. Anal. Calorim.* **98**, 309 (2009).
- [19]. A. Ray, A. Banerjee, A. Dubey, *Int. J. Agric. Environ. Biotechnol.* **13**, 423 (2020).
- [20]. Y.S. Yun, M.H. Park, S.J. Hong, M.E. Lee, Y.W. Park, H.J. Jin, *ACS Appl. Mater. Inter.* **7**, 3684 (2015).
- [21]. A. Lazzarini, A. Piovano, R. Pellegrini, G. Leofanti, G. Agostini, S. Rudić, M.R. Chierotti, R. Gobetto, A. Battiato, G. Spoto, A. Zecchina, C. Lambertiah, E. Groppo, *Catal. Sci. Technol.* **6**, 4910 (2016).
- [22]. S.K. Panigrahi, A.K. Mishra, *Photochem. Photobiol. Sci.* **18**, 583 (2019).
- [23]. A. Singh, P.K. Mohapatra, D. Kalyanasundaram, S. Kumar, *Mater. Chem. Phys.* **225**, 23 (2019).
- [24]. X. Li, H. Wang, Y. Shimizu, A. Pyatenko, K. Kawaguchi, N. Koshizaki, *ChemComm.* **47**, 932 (2011).
- [25]. N. Tarasenko, A. Stupak, N. Tarasenko, S. Chakrabarti, D. Mariotti, *ChemPhysChem* **18**, 1074 (2017).
- [26]. N. Enríquez-Sánchez, A.R. Vilchis-Nestor, S. Camacho-López, M.A. Camacho-López, M. Camacho-López, *Opt. Laser Technol.* **146**, 107591 (2022).

© 2024 by the authors; licensee SMCTSM, Mexico. This article is an open access article distributed under the terms and conditions of the Creative Commons Attribution license (<http://creativecommons.org/licenses/by/4.0/>).